Ab Initio Study of Hydrolysis of Amino Malononitrile: Formation of Amino Acetonitrile

Hong-Shun Zhu and Jia-Jen Ho*

Department of Chemistry, National Taiwan Normal University, 88, Section 4, Tingchow Road, Taipei, Taiwan 117, Republic of China

Received: February 7, 2001; In Final Form: April 23, 2001

Ab initio theoretical calculation was carried out to study the hydrolysis of amino malononitrile. The proposed scheme was considered as one of the possible reaction paths that the simplest amino acid, glycine, may be synthesized by the nature. Several other probable schemes based on the potential reaction sites of amino malononitrile were also examined. The optimized structures of the species on the reaction potential energy surfaces in addition to the activation energies were calculated at both HF and MP2 levels. The basis set superposition error (BSSE) for the correction of calculated energy was also performed. It came out that one of the proposed reactions had the lower potential energy profile in the sequential processes to form the amino acetonitrile. Most of the calculated barriers in this scheme were below 60 kcal/mol. The first added H_2O in the hydrolysis of amino malononitrile was calculated to be at lower barrier (49.00 kcal/mol) on attacking one of the nitrile group of amino malononitrile and successively forming an amide, rather than attacking on the amino group of amino malononitrile (82.24 kcal/mol). Further frontier orbital analysis also proved the same fact. The second H_2O molecule was added to hydrolyze the forming amide and produced carboxylic acid, which then underwent decarboxylation to form amino acetonitrile. Direct decarboxylation needs around 61 kcal/mol to cross the barrier, the highest one in all the processes derived in Scheme 1. Of course, it may be assisted by the third molecule such as H_2O to lower the barrier (around 20 kcal/mol). From the calculated low barriers the proposed processes in Scheme 1 may be considered as one of the acceptable mechanisms in prebiotic chemical evolution on the primitive earth.

Introduction

Ever since he took the first steps toward a conscious life, Man has tried to solve the problems of cosmogony. The most complicated and also the most interesting of these is that of the origin of life. Many ideas on the origin of life stem from Oparin,[1] who argued that the spontaneous generation of the first living organism might reasonably have taken place if large quantities of organic compounds had been present in the oceans of the primitive earth. Oparin further proposed that the atmosphere was reducing and that organic compounds might be synthesized under these conditions.[1−3] The pre-biotic evolution was explored in the classic experiments of Miller,[4] in 1953, and in many later experiments.[5−30] Miller took a plausible reducing atmosphere composed of methane, ammonia, molecular hydrogen, and water vapor, then passed electric sparks through it and collected the reaction products. He found a mixture of organic compounds containing a remarkably high fraction of amino acids. Other people have repeated the Miller experiments with many variations, using thermal energy,[10−17] ultraviolet light,[18−25] or ionizing radiation[26−30] as the energy source instead of electric spark. The results were always consistent. The upshot of Miller's experiments was that we could rely on nature to provide an ample supply of amino acids on the primitive earth.

The experiments using thermal energy have not been as complete or detailed as they have been for electrical discharge, but they have been somewhat more detailed than for the ultraviolet light.[31] The suggestion was that amino acid (glycine) came from the amino malononitrile, $NH_2CH(CN)_2$, by a complete hydrolysis of one of the nitriles, to give the carboxylic acid, which could decarboxylate and give amino acetonitrile:

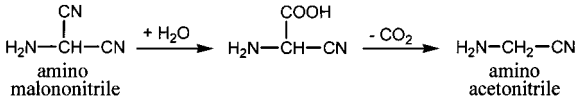

This could be either hydrolyzed to form glycine or polymerized to form polyglycinimide. Further hydrolyzation of the latter could give a polyglycine derivative that was the first real peptide, or protein, in chemical evolution.

In this present study, we applied ab initio quantum chemical methods to evaluate every steps of the mechanism starting from the reaction of amino malononitrile plus water molecule, including several possible branching processes for this reaction. We described the structures, hydrogen-bonding interactions, and potential energy surfaces (PES) of each stationary point in the relevant reaction paths.

Methods of Calculation. The ab initio calculation was performed for complete geometry optimization at both the restricted Hartree−Fock (RHF) and second-order Møller−Plesset (MP2) levels on either a Digital DEC-433au or SGI Origin 2000 workstation by using the Gaussian98[32] suite of programs. Optimizations of minima as well as transition structures were carried out with triple-ζ type basis sets including polarization functions (TZP), 6-311G(d,p). At the same level of theory, frequency calculations were performed in order to identify the stationary points as local minima, transition structures or higher order saddle points on the PES, and the thermodynamic properties, respectively. All the stationary points have been positively identified for minimum (number of

* Corresponding author. Address: Department of Chemistry, National Taiwan Normal University, 88, sec. 4, Tingchow Rd. Taipei, Taiwan 117, ROC. Phone: (886)-2-29309085. Fax: (886)-2−29324249. E-mail: jjh@scc.ntnu.edu.tw.

10.1021/jp010455q CCC: $20.00
Published on Web 06/13/2001

SCHEME 1

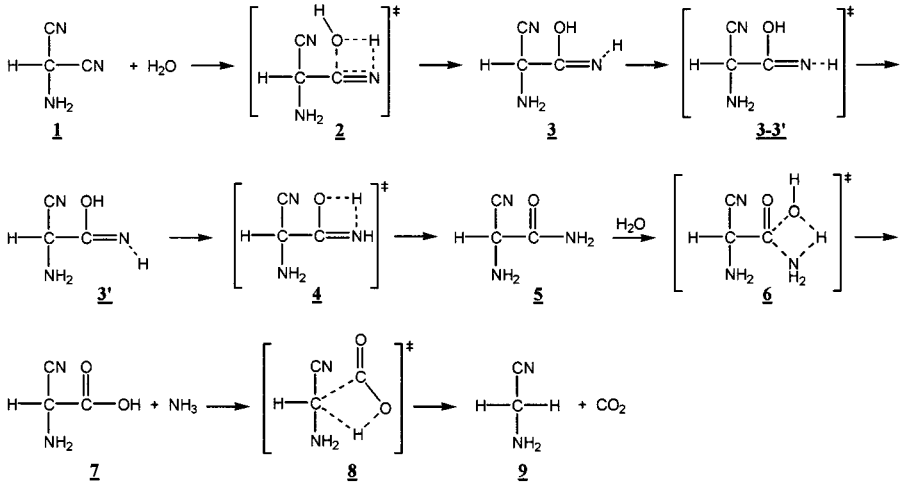

imaginary frequencies NIMAG = 0) or transition state (NIMAG = 1). Intrinsic reaction coordinate (IRC) calculations were also performed to ensure the transition states at the desired reaction coordinate at HF/6-311G(d,p). The calculated energies were corrected for zero-point vibrational energy (ZPVE) with the scaling factor of HF being 0.9248 and MP2 0.9748.[33] We also performed the Natural Population Analysis (NPA) of charge and Wiberg bond index (WBI)[34] by using the NBO program[35,36] in Gaussian98 at MP2 level. The basis set superposition error (BSSE) inherent in the computation of molecular interaction energies was corrected via the Boys−Bernardi counterpoise technique.[37] The frontier molecular orbitals obtained from MP2/6-31G** results were plotted using the Molden v3.6 program written by G. Schaftenaar.[38]

Results and Discussion

There were two potential reaction sites (CN and NH_2) in amino malononitrile to which the water molecules could be added. Each leads to its own mechanisms and reaction intermediates. In this study we first derived the reaction mechanism of the formation of amino acetonitrile from the hydrolysis of amino malononitrile, labeled Scheme 1, which was in accord with the formation process of glycine from amino malononitrile predicted by Calvin.[31]

The geometric structure and parameters of each species in the proposed mechanism are drawn in Figure 1 (**1**−**9** compounds). A number is assigned underneath each structure as a notation of the species. Each odd number represents a local minimum on the potential energy surfaces while the even number a transition state on the surfaces. Amino malononitrile, labeled **1**, has two local conformers, one with C_1 symmetry (more stable by 2 kcal/mol) than the other, C_s. We found that there existed a hyperconjugation effect[39] occurring between the lone pair electrons of the nitrogen atom and the antibonding orbital of σ^*_{C2-C6} in the C_1 conformer as well as in the C_s counterpart occurring between the lone pair electrons of the nitrogen atom and the antibonding orbital of σ^*_{C2-H1}. The schematic diagrams of Newman projection were shown below.

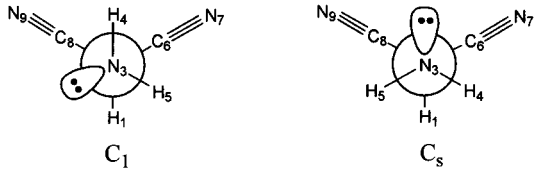

The NBO analysis of the C_1 conformer showed that the calculated hyperconjugation energy was 12.3 kcal/mol, which resulted in the increase of the C_2-C_6 bond length to 1.483 Å as compared to the analogous bond length of the C_2-C_8, 1.470 Å, while it was only 11.2 kcal/mol in the C_s counterpart, and the C_2-H_1 bond length also increased from 1.096 to 1.101 Å. If we turn the C_2-N_3 bond of **1** to shift between conformers then the variation of calculated activation energies with respect to the torsional angles of $\angle H_4N_3C_2H_1$ is drawn below. The

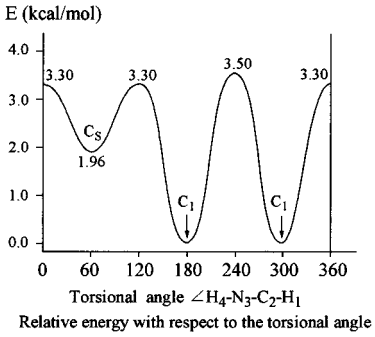

Relative energy with respect to the torsional angle

activation energies needed for the transformation of these conformers are not very high (less than 4 kcal/mol) and we choose the C_1 conformer, the most stable conformation on the diagram, for later calculations.

Addition of H_2O onto the CN Group. The O atom of the first added H_2O was positioned near the carbon while the H atom to the N atom of the nitrile group of amino malonomitrile, **1**, and a transition structure **2** was generated. It contained a four-membered ring, see Figure 1, and the bond distance between O_{10} and C_8 was 1.706 Å, the bond order 0.50, and that between H_{11} and N_9 was 1.361 Å and 0.34, respectively. While the bond between C_8 and N_9 extended from 1.174 Å to 1.219 Å and the bond order decreased from 2.93 to 2.27 (triple bond degrading to a double bond), and that of the $O_{10}-H_{11}$ bond extended to 1.262 Å, the bond order decreased to 0.31. The calculated NPA charge of H_{11} was 0.54; therefore, it was more like a proton than a hydrogen transfer. The transfer of a proton from H_2O molecule to the nitrile group was complete and formed a hydroxy imine, structure **3**. Its dihedral angle $\angle O_{10}C_8N_9H_{11} = -2.2°$, which makes O_{10}, C_8, N_9, and H_{11} four atoms near a plane. The lone-pair p orbital of O_{10} can then be parallel to the C_8-N_9 π orbital, and further stabilizes the hydroxy imine structure. The schematic structure is shown below.

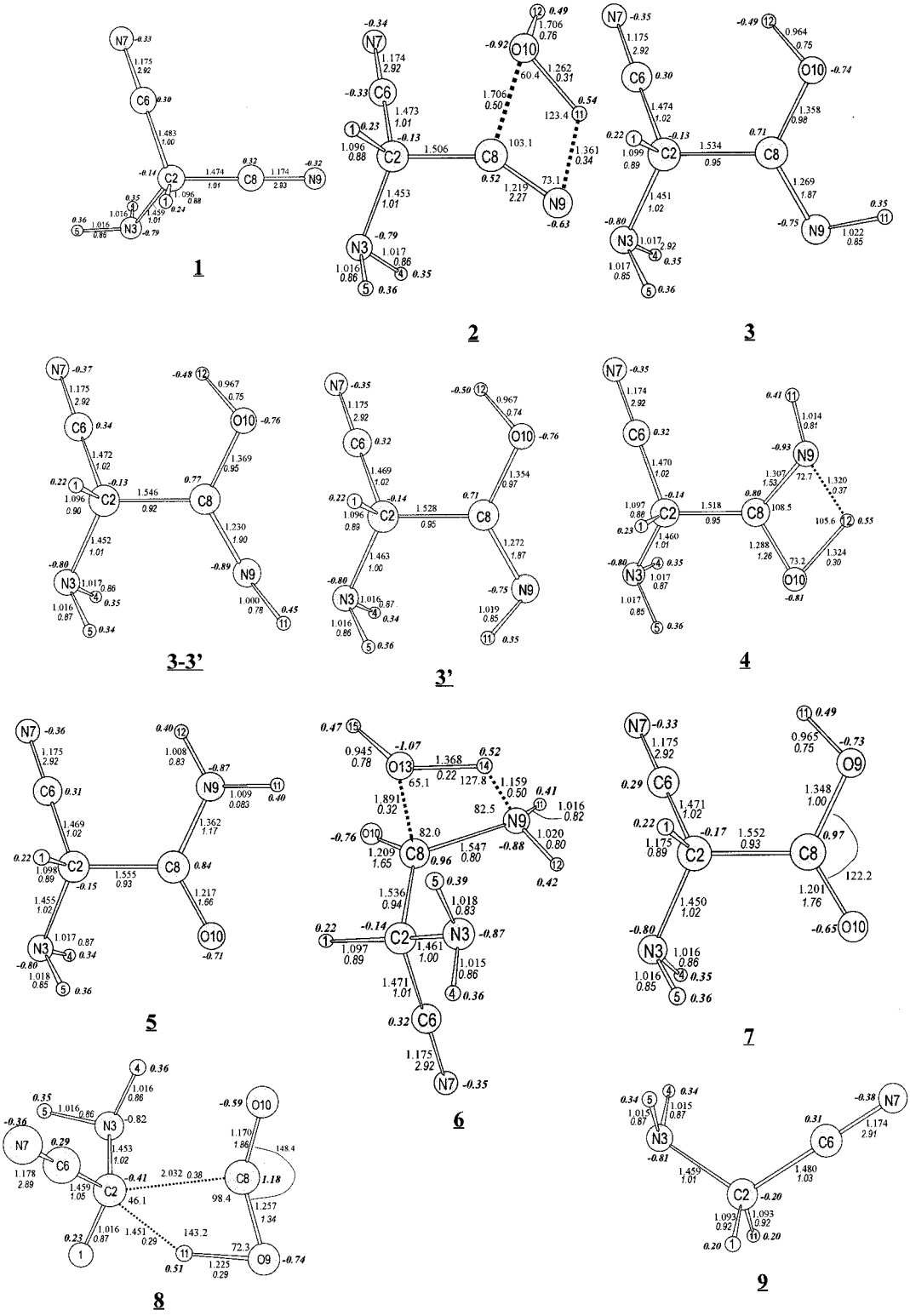

Figure 1. The calculated optimized structures, identified with a number underneath in accord with the species in reaction Scheme 1, are plotted, respectively. The bond distances (in angstroms), angles (in degrees), bond orders (italic), and atomic charges (bold) are labeled directly in the corresponding positions.

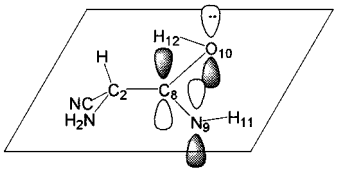

Energetically, the calculated activation energy of the hydration of **1** via transition structure **2** to form **3**, is 69.43 kcal/mol at HF, but only 49.00 kcal/mol at MP2. This large difference between the calculated HF and MP2 results indicates that the correlation energy was enhanced in the calculation for the structures involving new bond formation or destruction. Since there is still one lone-pair electrons on the N_9 atom of structure **3**, an intramolecular hydrogen transfer from the hydroxy group may take place. The hydrogen on the imine group may shift via **3**−**3′** to **3′** (without turning the C═N double bond) with

SCHEME 2

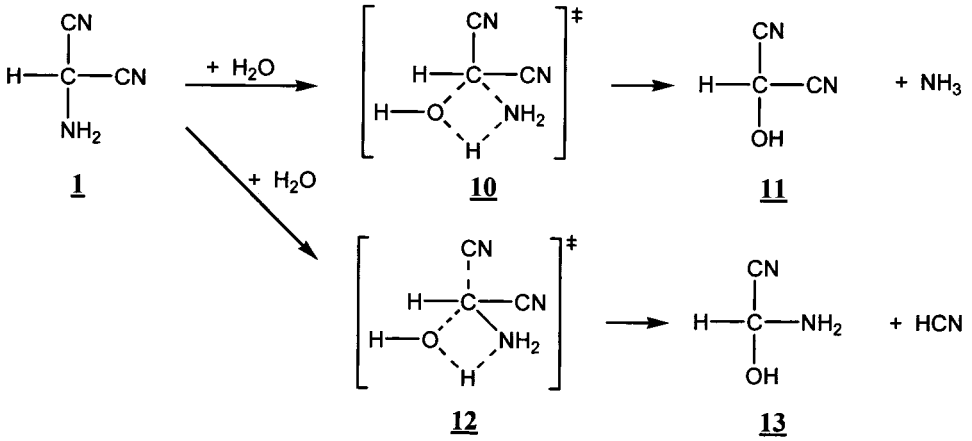

the calculated activation energy being 22.35 at HF and 21.38 kcal/mol at MP2. Here the difference between the calculated HF and MP2 is not significant due to no bond changes between structures **3** and **3′**. The H_{12} atom may transfer from O_{10} to N_9 (via the transition structure **4**) and forms an amide, **5**. The NPA calculation for the charge of H_{12} is 0.55, also more like a proton transfer with the calculated activation energy being 31.02 kcal/mol (44.31, HF), and largely exothermic. A NBO calculation showed a strong hyperconjugated interaction (energy as high as 62.95 kcal/mol) between the lone-pair electrons of N_9 atom and the antibonding orbital of $\pi^*_{C_8-O_{10}}$ in structure **5** and resulting in a shorter bond length of C_8-N_9 than a normal single C−N bond, only 1.362 Å compared to a normal 1.455 Å, and a greater bond order, 1.17, than that of a single bond. Structure **5** is more stable than **1** by 24.12 kcal/mol calculated at MP2 level, indicating that **5** is a stable intermediate and would possibly be observed during the reaction.

Addition of Second H_2O. One of the hydrogens of H_2O may move to the nitrogen end of amide and that of O atom of H_2O forms bonding with the C atom of amide and a transition structure of **6** may be obtained. Further elimination of one NH_3 molecule from **6** a carboxyl structure **7** would be formed. Before elimination, a graduate weaker C_8-N_9 bond (bond distance extended from 1.362 to 1.547 Å and the bond order decreased from 1.17 to 0.80) and a graduate strengthen bonds of C_8-O_{13} and N_9-H_{14} were observed (bond distance and bond order of the former were 1.891 Å and 0.32, while for the latter 1.159 Å and 0.50). The $O_{13}-H_{14}$ bond distance also became larger, 1.368 Å, with decreased bond order 0.22. All these conditions speeded up the transfer of H_{14} from O_{13} to N_9 and the detachment of the NH_3 molecule became unavoidable. Energetically, our calculation showed impressive low activation energy in this process, compared to that of the first added H_2O. It was only 44.55 kcal/mol at MP2 and 56.60 kcal/mol at HF.

Further Elimination of CO_2. An intramolecular hydrogen transfer[40,41] in carboxyl compound **7** would take place if we shorten the distance between H_{11} and C_2. H_{11} departed from O_9 and move to C_2 and simultaneously broke the C_2-C_8 bond to release a CO_2. The transition structure **8** was obtained for this process with the distance between C_2 and C_8 increasing from 1.552 Å (of **7**) to 2.032 Å, and the bond order decreasing from 0.93 to 0.38. The distance between H_{11} and O_9 also increases to 1.225 Å. Further analysis we found that the angle $\angle O_9C_8O_{10}$ (of **8**) increased from 122.2° (of **7**, sp^2 type) to 148.4° and finally to a near sp type hybridization (CO_2) plus the formation of structure **9**. The energy barrier for this process was calculated to be 61.08 kcal/mol (82.47, HF), a little bit high. However, it released quite a lot of heat −75.32 kcal/mol (MP2) from the barrier to the product. The enthalpy change for the overall reaction from **1** to **9**, i.e., $\mathbf{1} + 2H_2O \rightarrow \mathbf{9} + CO_{2(g)} + NH_{3(g)}$ was −32.94 kcal/mol (−40.49, HF) with structure **9** being the most stable compound in Scheme 1.

As described in the former section,amino malononitrile may have more than one reaction site for the addition of H_2O, as described in Scheme 2. The O atom of the added H_2O was connected to the central carbon atom of **1**, and one of the H atoms to the N atom of the amino group. A transition structure **10** was obtained, see Figure 2, in which the C_2-N_3 bond was about to break and finally form structure **11** plus one NH_3 molecule. The other alternative in Scheme 2 led to transition structure **12** in which the C_2-C_6 bond started to extend and finally form structure **13** plus one HCN molecule via **13-complex**. The latter mechanism is more like a reverse-attack substitution reaction. Our calculation showed that if the incoming angles of H_2O with each of the two CN groups in **1** were smaller than 180°, as depicted in **10**, then the resultant products would be structure **11** plus one NH_3 molecule. In contrast, if the incoming angles were almost close to 180°, such as in structure **12** ($\angle O_{10}C_2C_6 = 171.3°$), then a reverse substitution reaction would take place. In structure **10** the angles of incoming H_2O with the two CN groups were $\angle O_{10}C_2C_8 = 151.1°$ and $\angle O_{10}C_2C_6 = 93.4°$, much smaller than 180°, and it initiated the bond formation of C_2-O_{10} and $H_{12}-N_3$ but the bond dissociation of C_2-N_3 and $O_{10}-H_{12}$. The distance between C_2 and O_{10} started to decrease, 2.048 Å and the bond order 0.30, as well as the distances of H_{12} to N_3 1.068 Å and 0.64 bond order. In contrast, the distance between C_2 and N_3 increased from 1.459 to 2.000 Å and the bond order decreased from 1.01 to 0.54, so did the distance of O_{10} to H_{12} increase to 1.521 Å and bond order decrease to 0.12. While in structure **12** the attack of H_2O forms the angle $\angle O_{10}C_2C_6 = 171.3°$, very close to 180°, and the dihedral angle $\angle H_1C_2C_8N_3 = 176.6°$, indicating that C_2, H_1, C_8, and N_3 atoms are almost in one plane. It is very alike a trigonal bipyramid structure with O_{10}, C_2, and C_6 atoms constituting the axis of the structure. The incoming H_2O and the leaving nitrile group are almost right on the opposite direction of the plane and make the reverse-substitution reaction occur easily. The reason that atoms O_{10}, C_2, and C_6 are not completely straight on one line may be due to weak intramolecular H-bonding between H_{12} and O_{10}, which pulls the O_{10} atom off the position. Energetically, the energy barriers for the processes in Scheme 2 are quite high, 82.24 and 82.34 kcal/mol, via **10** (release of NH_3) and via **12** (release of HCN),

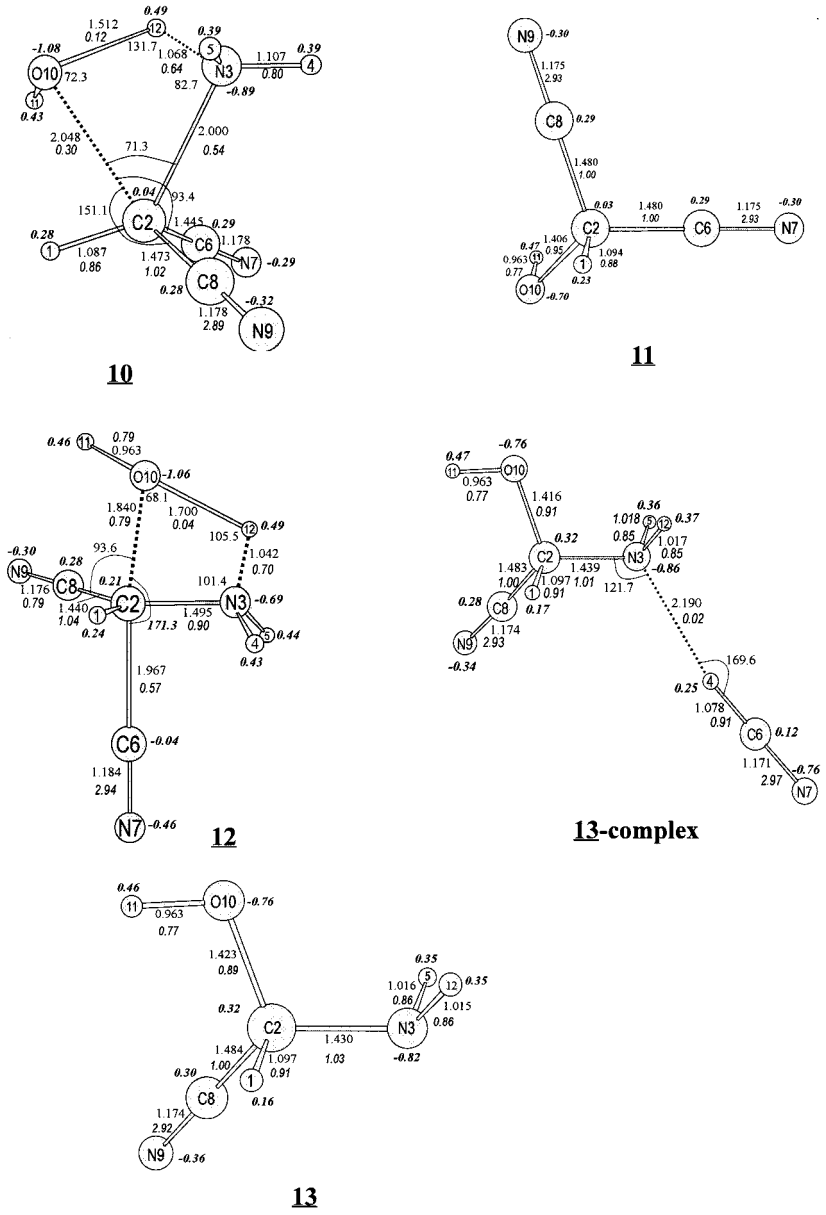

Figure 2. The calculated optimized structures, identified with a number underneath in accord with the species in reaction Scheme 2, are plotted, respectively. The bond distances (in angstroms), angles (in degrees), bond orders (italic), and atomic charges (bold) are labeled directly in the corresponding positions.

SCHEME 3

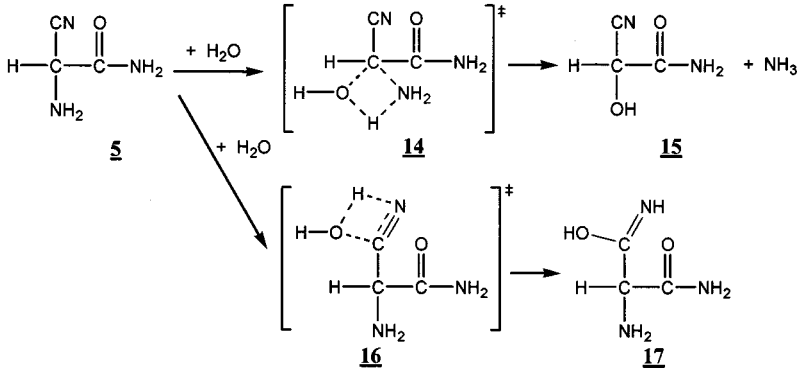

respectively, at MP2 (or 113.88 and 104.49 kcal/mol at HF), and are less likely to proceed in comparison with Scheme 1.

On the basis of the possible selection of the reaction sites, we also considered the alternative reaction scheme when the second H_2O molecule was added onto structure **5** to proceed further to the hydrolysis reaction. The possible scheme is shown in Scheme 3, and the calculated geometric parameters of structure **14** to **17** are plotted in Figure 3. The added second H_2O molecule may choose to form bonding with the amino group or nitrile group in **5**, to generate the transition structures

SCHEME 4

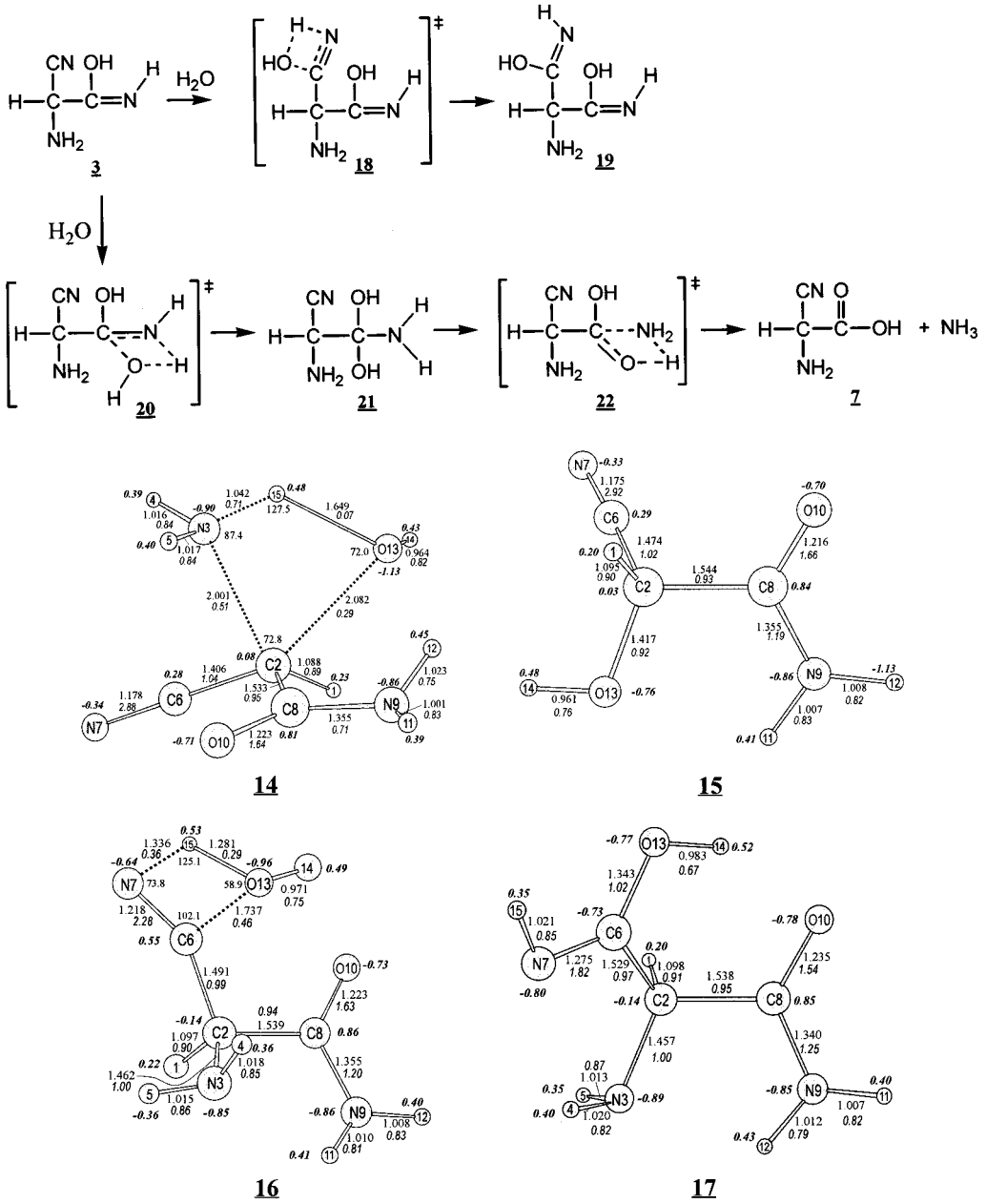

Figure 3. The calculated optimized structures, identified with a number underneath in accord with the species in reaction Scheme 3, are plotted, respectively. The bond distances (in angstroms), angles (in degrees), bond orders (italic), and atomic charges (bold) are labeled directly in the corresponding positions.

14 and **16**, respectively. The choice via **14** has the O_{13} atom of added H_2O connected to C_2 and of H_{15} to N_3 atom. Consequently, the bond distance of $H_{15}-O_{13}$ increases to 1.649 Å and the bond order decreases greatly to 0.07, indicating a bond breaking of $H_{15}-O_{13}$ and a simultaneously bond formation of $H_{15}-N_3$, bond distance 1.042 Å and 0.71 bond order. The final product of this process is structure **15** associated with a release of NH_3 molecule, and an energy barrier of 78.01 kcal/mol (105.59, HF), very close to that of the process (via **10**) described in Scheme 2. The other process (via **16**) is the addition of H_2O onto the nitrile group with the connections of O_{13} of H_2O to C_6 and H_{15} to N_7. The calculated bond lengths and bond orders for these bondings in the transition structure are indicated in the figure and are similar to those obtained in structure **2** of Scheme 1. The calculated energy barrier is 46.95 kcal/mol (68.71, HF), also close to that of the process of **1** + H_2O via **2** to form **3** described in Scheme 1. Since there is only minor structure difference between **1** and **5** (one of the nitrile groups in **1** being replaced by an amide group), they exhibit very close energy barriers while they form near hydrated transition structures, such as **10** and **14** (addition of H_2O onto the amino group), and **2** and **16** (addition of H_2O onto the nitrile group). Structure **17**, product via **16**, containing three functional groups: one amide, one amino, and one hydroxy imine, has three types of intramolecular hydrogen bonding. They are $N_3\cdots H_{12}$, $O_{10}\cdots H_{14}$, and $N_7\cdots H_4$, with interdistances and bond orders of [2.106 Å, 0.01], [1.746 Å, 0.05], and [2.105 Å, 0.01], respectively. The hydrogen atom having H-bonding in the molecule always has relative more positive charges. For example, the calculated NPA charge of H_4 is 0.40, higher than H_5 of 0.35, and the charge of H_{12} is 0.43, higher than H_{11} of 0.40, and that of H_{14} is 0.52, the strongest intramolecular H-bonding in the molecule. To form better intramolecular hydrogen bonding, some related single bonds twist to an angle such that the direction of lone-pair orbital

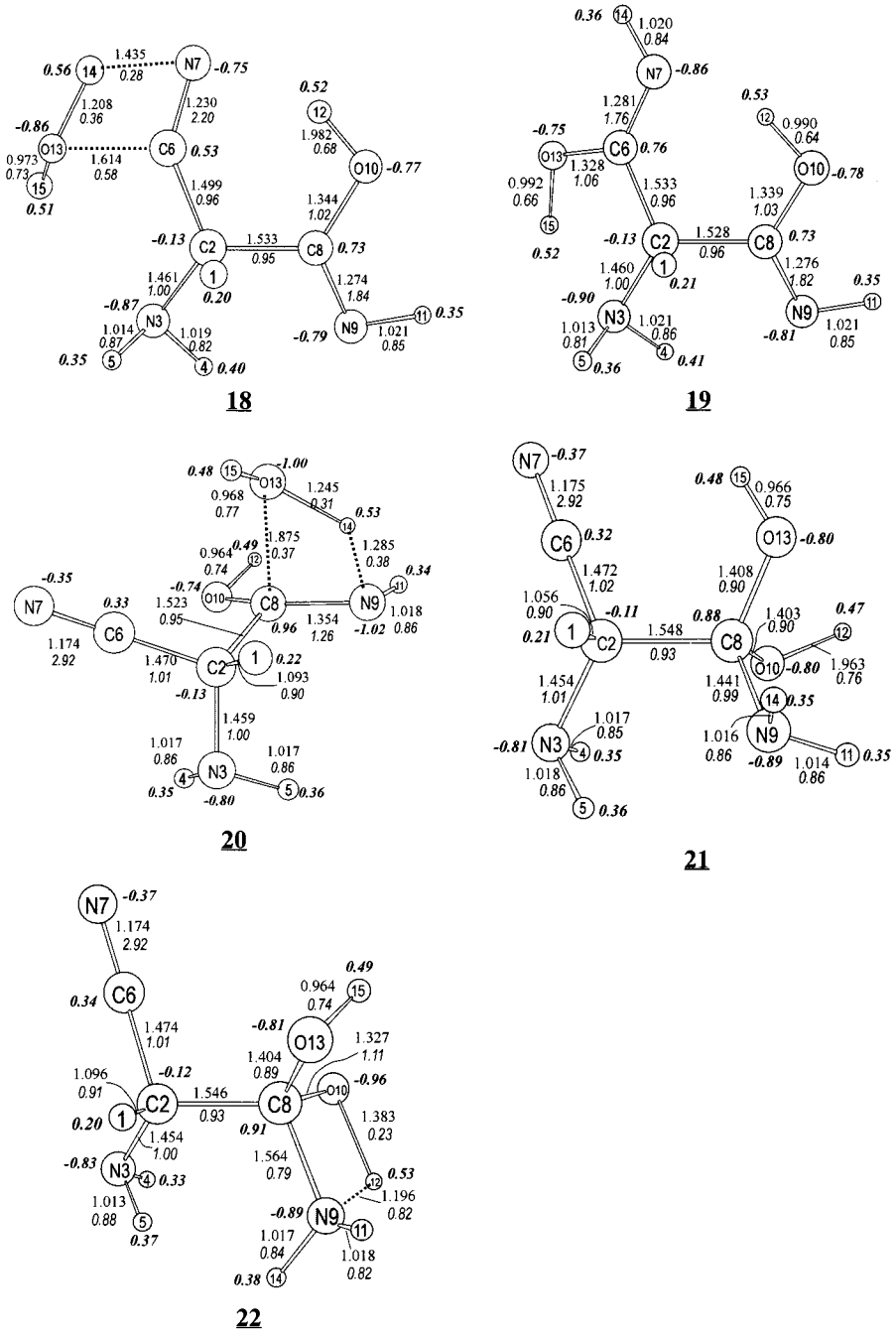

Figure 4. The calculated optimized structures, identified with a number underneath in accord with the species in reaction Scheme 4, are plotted, respectively. The bond distances ((in angstroms), angles (in degrees), bond orders (italic), and atomic charges (bold) are labeled directly in the corresponding positions.

of N or O atom has better overlap with the hydrogen orbital. For example, the single bond C_2-N_3 in **17** has the lone-pair orbital of N_3 facing H_{12} in addition to letting the orientation of H_4 be more parallel to the lone-pair direction of N_7. The twisting of the C_6-O_{13} bond to let H_{14} meet the best overlap orientation of lone-pair orbital of O_{10} can also be expected. However, to twist the C_6-N_7 bond needs more energy since it is a double bond. A comparison of intramolecular hydrogen bonding of $N_7\cdot\cdot\cdot H_4$ (2.105 Å, 0.01 bond order) in **17** with that of $N_3\cdots H_4$ in **13-complex** (2.190 Å, 0.02 bond order) further shows the significance of the appropriate orientation of the lone-pair orbital on the nitrogen atom toward the hydrogen. Although with a shorter distance (2.105 Å to 2.190 Å) but not suitable lone-pair orientation due to large twisting barrier of C═N double bond in $N_7\cdots H_4$ (**17**), the H-bonding strength is still smaller (0.01 to 0.02 bond order) than that in $N_3\cdots H_4$ (**13-complex**), which has a proper lone-pair orientation.

Two other branching reactions that possibly occur at the addition of the second H_2O on structure **3** were depicted in Scheme 4.

One is the addition onto the nitrile group of **3** via transition structure **18** to form **19**. The other is the addition of H_2O onto the hydroxy imine group via transition structure **20** to form an intermediate **21**, and then through intramolecular hydrogen transfer passing the transition structure **22** to form **7** plus one NH_3 molecule. The focus part of transition structure **18** is very alike to **2** and **16** in Schemes 1 and 3, which results in the formation of similar portion in the products **19**, **3**, and **17**. C_6, N_7, H_{14}, and O_{13} of **18** in Figure 4 form a four-membered ring with the distance and bond order between O_{13} and C_6 being

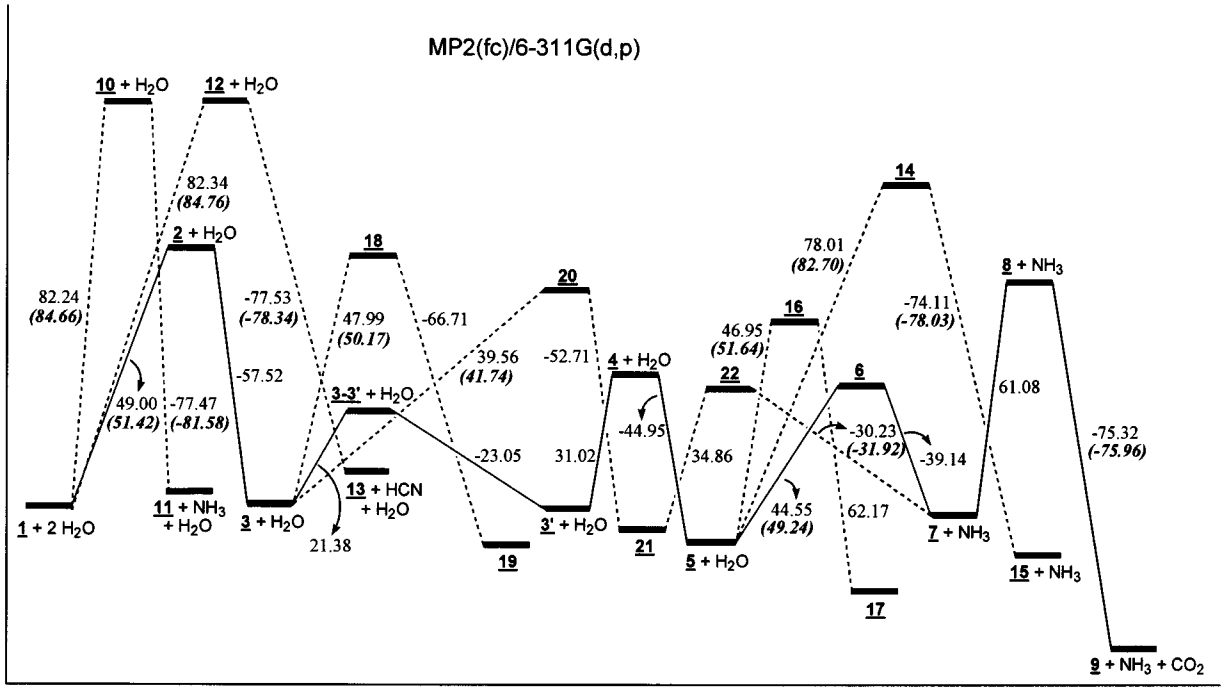

Figure 5. Potential energy diagram containing all the possible optimized species in schemes 1 to 4 is plotted with respect to their relative energies (kcal/mol) on the potential energy surfaces. The activation energy for each process is indicated on the left slant dotted line, while on the right the release of energy to the product from its corresponding transition structure. The full slant line represents the processes of Scheme 1. The included BSSE correction energy is also indicated in the parentheses (bold).

1.614 Å and 0.58, while that of H_{14} to O_{13} 1.208 Å and 0.36, H_{14} to N_7 1.435 Å and 0.28, indicating that the added second H_2O forms bonding with the nitrile group and ready to produce a hydroxy imine structure of **19**. The dihedral angle $\angle H_{15}O_{13}C_6N_7 = 177.79°$, so that the lone-pair p orbital of O_{13} can be parallel to the $\pi_{C_6=N_7}$ orbital and generates a hyperconjugation interaction to stabilize the structure. The other part of the structure, N_9, C_8, O_{10}, also has a similar stabilization effect further lower down the structure. In addition, there are two major intramolecular H-bondings in **19**, $N_3\cdots H_{15}$ and $N_7\cdots H_{12}$, with bond distance and bond order [1.797 Å, 0.06], and [1.772 Å, 0.07], respectively, to lower the energy. It may also contribute to the appropriate orientations along C_2-N_3, C_2-C_6 and C_2-C_8 bonds to make better H-bonding interactions. The activation energy for this process was calculated to be 47.99 kcal/mol (70.88, HF). The other possible branching reaction via **20** needs less energy, 39.56 kcal/mol (57.88, HF), to cross the barrier and produce **21** which has one nitrile group, two hydroxy groups, and one amino group, but **21 is** not that stable. Furthermore, there was no intramolecular H-bonding interaction in the optimized geometry due to sp^3 hybridization in the C_2 and C_8 orbital-bonding structures. It is possible to proceed intramolecular hydrogen transfer of H_{12} to N_9 through the transition structure **22** to form product **7** plus one NH_3 molecule. The calculated activation energy was as low as 34.86 kcal/mol (47.81, HF), lower than the latent heat (−52.71 kcal/mol at MP2) from the preceding process forming **21** from **20**.

Energy Profile. All the species on the stationary points of the potential energy surfaces in Schemes 1−4 are plotted against their relative energies in Figure 5, calculated at MP2/6-311G-(d,p) after thermal free energy and zero point energy corrections (including frequency scaling factor).[33] The calculated energy including BSSE correction was also given in the parentheses. The calculated energies at HF and MP2 levels for all the mentioned species are listed in Table 1. The BSSE correction energies (kcal/mol) calculated at HF and MP2 levels are listed in Table 2. As shown in the figure, the lower energy profile follows the processes in Scheme 1 containing species **1** → **9**. Processes in Scheme 2, alternative reaction paths on the addition of H_2O resulting in removing NH_3 or HCN, need much higher activation energies, 82.24 and 82.34 kcal/mol, respectively, as compared to 49.00 kcal/mol in Scheme 1. Further analysis from frontier orbital theory also proves that Scheme 1 is more favored. As shown in Figure 6 the calculated HOMO of H_2O is mainly a $2p_z$ orbital with a plane of symmetry, while the LUMO of **1** an extended π-symmetry on the NC−C−CN chain together with two terminal lone-pair orbitals from nitrogen atoms and a lone-pair orbital from amino group. Phase symmetry and the overlap magnitude of the frontier orbitals are crucial factors for the

TABLE 1: Sum of the Calculated Electronic and Zero-Point Energies (au) of All Species at HF/6-311G(d,p) and MP2 (fc)/6-311G(d,p) Levels

	HF	MP2		HF	MP2
01	−278.670348	−279.589614	**11**	−298.512094	−299.449981
02	−354.585365	−355.754218	**12**	−354.529494	−355.70109
03	−354.705443	−355.845874	**13**	−261.807695	−262.638358
03−03′	−354.669822	−355.811800	**14**	−430.590173	−431.989109
03′	−354.708197	−355.848537	**15**	−374.577123	−375.732498
04	−354.637588	−355.799099	**16**	−430.648939	−432.038605
05	−354.732775	−355.870736	**17**	−430.773650	−432.137676
06	−430.668244	−432.042423	**18**	−430.620900	−432.014754
07	−374.571400	−375.730080	**19**	−430.750075	−432.121057
08	−374.439982	−375.632735	**20**	−430.641622	−432.028180
09	−186.933936	−187.564985	**21**	−430.745964	−432.112176
10	−354.514526	−355.701242	**22**	−430.669767	−432.056616
H2O	−76.025660	−76.242687	**CO2**	−187.675689	−188.187776
NH3	−56.176575	−56.374718	**HCN**	−92.8834800	−93.1862800

TABLE 2: Calculated BSSE Corrected Energies (kcal/mol)

	HF	MP2		HF	MP2
1 + H_2O	−0.96	−2.42	**9** + CO_2	−0.23	−0.64
3 + H_2O	−0.60	−2.18	**11** + NH_3	−1.98	−4.11
5 + H_2O	−2.13	−4.69	**13** + HCN	−0.30	−0.81
7 + NH_3	−0.85	−1.69	**15** + NH_3	−1.87	−3.92

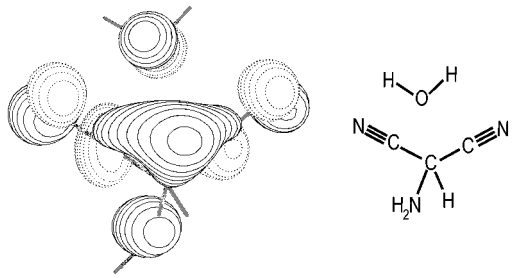

Figure 6. The shape and phase of calculated frontier orbitals of HOMO of H_2O (contour spacing 0.1500) and LUMO of amino malononitrile (contour spacing 0.0600) are plotted at MP2/6-31G**.

reaction to proceed. The added H_2O has its HOMO same symmetry as the central region of LUMO of **1**, which leads the addition of H_2O onto the CN group more directly and with lower energy profile as compared to the addition onto the NH_2 group. Therefore, processes in Scheme 1 are reasonable reaction paths for the hydrolysis of amino malononitrile in this study.

Conclusion

So far we have calculated and demonstrated part of the reasonable schemes for the hydrolysis of amino malononitrile to produce glycine as a final product (right now we have reached species **9**, amino acetonitrile). We came to the conclusion that the mechanism in Scheme 1 was the most favorable pathway determined by HF and MP2 calculations. All of the reaction barriers for the Scheme 1 are below 62 kcal/mol. The addition of H_2O molecule onto the nitrile group of amino malononitrile will be the first step of the whole scheme. Our next strategy will be a continuation of the reaction scheme from **9** to the formation of glycine.

Acknowledgment. Support for this research from the National Science Council of the Republic of China (NSC-89-2113-M-003-023) is gratefully acknowledged. We are also grateful to the National Center for High-Performance Computing where the Gaussian package and the computer time were provided. We are also indebted to the reviewers for their helpful suggestions concerning the manuscript.

References and Notes

(1) (a) Oparin, A. I. *The Origin of Life;* MacMillan: New York, 1938. (b) Oparin, A. I. *Origin of Life*; 1924 [Reprinted from Bernal, J. D. *Origin of Life*; Weidenfeld & Nicolson: London, 1967, pp 199−234.].

(2) Urey, H. C. *The Planets, Their Origin and Development;* Yale University Press: New Haven, CT, 1952; Chapter 4.

(3) Bernal, J. D. *Proc. Phys. Soc.* **1949,** *62A*, 537; **1949,** *62B*, 597.

(4) Miller, S. L. *Science* **1953**, *117*, 528−529.

(5) Miller, S. L. *J. Am. Chem. Sec.* **1955**, *77*, 2351.

(6) Miller, S. L. *Biochim. Biophys, Acta* **1957**, *23*, 480.

(7) Abelson, P. H. *Science* **1956**, *124*, 935.

(8) Pavlovskaya, T. E.; Passynsky, A. G. *Reports of the Moscow Symposium on the Origin of Life* Aug 1957, 98.

(9) Heyns, K.; Walter, W.; Meyer, E. *Naturwissenschaften* **1957**, *44*, 385.

(10) Urey, H. C. *Proc. R. Soc.* (London) **1953**, *219A*, 281.

(11) Fox, S. W.; Johnson, J. E.; Vegotsky, A. *Science* **1956**, *124*, 923.

(12) Fox, S. W.; Johnson, J. E.; Vegotsky, A. *Ann. N. Y. Acad. Sci.* **1957**, *69*, 328.

(13) Fox, S. W.; Johnson, J. E.; Vegotsky, A. *J. Chem. Educ.* **1957**, *34*, 472.

(14) For a review, see: Katchalski, E. *Adv. Protein Chem.* **1951**, *6*, 123.

(15) (a) Harada, K.; Fox, S. W. *J. Am. Chem. Soc.* **1958**, *80*, 2694. (b) Vegotsky, A.; Harada, K.; Fox, S. W. *J. Am. Chem. Soc.* **1958**, *80*, 3361.

(16) Fox, S. W.; Harada, K. *Science* **1958**, *128*, 1214.

(17) Abelson, P. H. *Ann. N. Y. Acad. Sci.* **1957**, *69*, 276.

(18) Miller, S. L. *Ann. N. Y. Acad. Sci.* **1957**, *69*, 260.

(19) Groth, W. *Angew. Chem.* **1957**, *69*, 681..

(20) Groth, W.; von Weyssenhoff, H. *Naturwissenschaften* **1957**, *44*, 510.

(21) Terenin, A. N. *Reports of the Moscow Symposium on the Origin of Life* Aug **1957**, 97.

(22) Ellenbogen, E. *Abstr. Am. Chem. Soc. Meeting, Chicago* **1958**, 47C.

(23) Bahadur, K. *Nature* **1954**, *173*, 1141.

(24) Bahadur, K. *Nature* **1958**, *182*, 1668.

(25) Pavlovakaya, T. E.; Passynsky, A. G. *Int. Congr. Biochem. 4th Congr. Abstr. Commun.* **1958**, 12.

(26) Dose, K.; Rajewsky, B. *Biochim. Biophys. Acta* **1957**, *25*, 225.

(27) Hasselstrom, T.; Henry, M. C. *Science* **1956**, *123*, 1038.

(28) Garrison, W. M. et al. *J. Am. Chem. Soc.* **1953**, *75*, 2459.

(29) Hasselstrom, T.; Henry, M. C.; Murr, B. *Science* **1957**, *125*, 350.

(30) Paschke, R.; Chang, R.; Young, D. *Science* **1957**, *125*, 881.

(31) Calvin, M. *Chemical Evolution, Molecular Revolution towards the Origin of Living Systems on the Earth and Elsewhere*; Clarendon Press: Oxford, 1969.

(32) Frisch, M. J.; Trucks, G. W.; Schlegel, H. B.; Scuseria, G. E.; Robb, M. A.; Cheeseman, J. R.; Zakrzewski, V. G.; Montgomery, J. A.; Stratmann, R. E.; Burant, J. C.; Dapprich, S.; Millam, J. M.; Daniels, A. D.; Kudin, K. N.; Strain, M. C.; Farkas, O.; Tomasi, J.; Barone, V.; Cossi, M.; Cammi, R.; Mennucci, B.; Pomelli, C.; Adamo, C.; Clifford, S.; Ochterski, J.; Petersson, G. A.; Ayala, P. Y.; Cui, Q.; Morokuma, K.; Malick, D. K.; Rabuck, A. D.; Raghavachari, K.; Foresman, J. B.; Cioslowski, J.; Ortiz, J. V.; Stefanov, B. B.; Liu, G.; Liashenko, A.; Piskorz, P.; Komaromi, I.; Gomperts, R.; Martin, R. L.; Fox, D. J.; Keith, T. A.; Al-Laham, M. A.; Peng, C. Y.; Nanayakkara, A.; Gonzalez, C.; Challacombe, M.; Gill, P. M. W.; Johnson, B. G.; Chen, W.; Wong, M. W.; Andres, J. L.; Head-Gordon, M.; Replogle, E. S.; Pople, J. A. *Gaussian 98*, Revision A.7; Gaussian, Inc.: Pittsburgh, PA, 1988.

(33) Scott, A. P.; Radom. L. *J. Chem. Phys.* **1996**, *100*, 16502.

(34) For applications of Wiberg bond indexes in analysis of various bonding patterns, for example, see: (a) Glukhovtsev, M. N.; Schleyer, P. v. R. *Chem. Phys. Lett.* **1992**, *198*, 547. (b) Wiberg, K. B. *Tetrahedron* **1968**, *24*, 1083. (c) Mayer, I. *Theor. Chim. Acta* **1985**, *67*, 315.

(35) (a) Reed, A. E.; Curtiss, L. A.; Weinhold, F. *Chem. Rev.* **1988**, *88*, 899−926. (b) Carpenter, J. E.; Weinhold, F. *J. Mol. Struct. (THEOCHEM)* **1988**, *169*, 41. (c) Foster, J. P.; Weinhold, F. *J. Am. Chem. Soc.* **1980**, *102*, 7211. (d) Reed, A. E.; Weinhold, F. *J. Chem. Phys.* **1983**, 1736. (e) Reed, A. E.; Weinstock, R. B.; Weinhold, F. *J. Chem. Phys.* **1985**, *83*, 735. (f) Reed, A. E.; Curtiss, L. A.; Weinhold, F. *Chem. Rev.* **1988**, *88*, 899.

(36) Glending, E. D.; Reed, A. E.; Carpenter, J. E.; Weinhold, F. NBO Version 3.1, implemented in Gaussian 98.

(37) Boys, S. F.; Bernardi, F. *Mol. Phys.* ***1970***, *19*, 553.

(38) Schaftenaar, G. *Molden*, version 3.6; CAOS/CAMM Center Nijmegen: Toernooiveld,Netherlands, 1991.

(39) Hehre, W. J.; Radom, L.; Schleyer, P. v. R.; Pople, J. A. *Ab initio Molecular Orbital Theory*; Wiley-Interscience: New York, 1986.

(40) (a) Chu, C.-H.; Ho, J.-J. *J. Phys. Chem.* **1995**, *99*, 1151. (b) Chu, C.-H.; Ho, J.-J. *J. Am. Chem. Soc.* **1995**, *117*, 1076. (c) Chu, C.-H.; Ho, J.-J. *J. Phys. Chem.* **1995**, *99*, 16590.

(41) (a) Wu, D.-H.; Ho, J.-J. *J. Phys. Chem. A.* **1998**, *102*, 3582. (b) Guo, J.-X.; Ho, J.-J. *J. Phys. Chem. A.* **1999**, *103*, 6433. (c) Yen, S.-J.; Ho, J.-J. *J. Phys. Chem. A.* **2000**, *104*, 8551. (d) Yen, S.-J.; Lin, C.-Y.; Ho, J.-J. *J. Phys. Chem. A.* **2000**, *104*, 11771.